

Responses of Radiation-Hardened Power MOSFETs to Neutrons

James E. Gillberg, *Member, IEEE*; Donald I. Burton, *Member, IEEE*; Jeffrey L. Titus, *Senior Member, IEEE*,
C. Frank Wheatley, *Life Fellow, IEEE*, and Noel Hubbard

Abstract - The test results of recent neutron irradiations performed on a variety of radiation-hardened power MOSFETs manufactured by Fairchild Semiconductor are reported here. Twelve device types from four different families with rated drain breakdown voltages from 30 to 500 volts of which most are n-channels and the others are p-channels, were characterized.

I. INTRODUCTION

MANY military and space systems are designed to operate in various radiation type environments. Potential radiation sources are neutrons and protons. Both of these radiation sources produce ionization and displacement damage. If the system and its individual components are not hardened to these radiation types and others, it could fail to operate properly or even cause catastrophic system failure.

Displacement damage is usually a low concern especially on components that are fabricated with highly doped, shallow junctions, which are used in most of today's complex integrated circuits. However, components that are widely used in almost every system are power MOSFETs. These devices incorporate a deep, lightly doped, epitaxial layer, which makes them more susceptible to displacement damage. Displacement damage can cause significant changes in a device's electrical performance such as increasing its on-resistance and breakdown characteristics or by changing its threshold voltage.

Many of the power MOSFET technologies that have been developed over the past ten years and currently being manufactured today have not been characterized to displacement damage effects. Therefore, a series of tests were designed to characterize displacement damage effects of several power MOSFET devices using different radiation-hardened families manufactured by Fairchild (formally Intersil). The first series of power MOSFETs exposed to neutrons at the Pennsylvania State University Breazeale TRIGA Mark III nuclear reactor are reported here. Using these test data, a preliminary database of displacement damage effects on power MOSFETs will be available to system designers. Data are provided in graphical format. Displayed points represent the average of the four samples of each device type exposed at the given neutron fluence.

Manuscript received July 17, 2001. This work co-sponsored by Fairchild Semiconductor and Defense Threat Reduction Agency (DTRA).

J. E. Gillberg is with the Fairchild Semiconductor, Somerville, NJ 08876 USA (telephone: 908-685-6236; e-mail: jim.gillberg@fairchildsemi.com)

D. I. Burton is with the Fairchild Semiconductor, 125 Crestwood Road, Mountaintop, PA 18707 USA

J. L. Titus is with NAVSEA Crane, 300 Highway 351, Crane, IN 47522-5001 USA (telephone: 812-854-1617, e-mail: jtitus@atd.crane.navy.mil).

C. F. Wheatley is a private consultant, 181 Middle Road, Drums, PA 18222 USA (telephone: 570-788-2319).

N. Hubbard is with NAVSEA Crane, 300 Highway 351, Crane IN 47522

II. TEST SETUP

One hundred ninety-two devices representing twelve different device types (16 samples for each device type) were provided by Fairchild in TO-39 type packages. All devices were electrically characterized prior to any neutron exposure by Fairchild. Four samples of each device type were provided to NAVSEA Crane as controls. The controls were used to correlate Fairchild test data and NAVSEA Crane test data. That correlation is not reported here. The other 12 samples of each device type were segmented into three groups of four, which were then placed into anti-static bags. These bags were then sent to Pennsylvania State University for neutron exposure.

Neutron exposures were performed using a "bag-type" test. Each bag was exposed to a specified level of neutrons, which was related to that device's rated drain breakdown voltage. Throughout this paper, neutron fluence is expressed in units of neutrons per square centimeter and is provided as a 1-MeV equivalent for silicon as determined by the dosimetry. Table 1 provides the device type, rated drain-to-source breakdown voltage (BV_{DSS}), channel type, and exposure levels.

TABLE 1: DESCRIPTION OF TESTED SAMPLES

Device Type	Rated BV_{DSS}	Channel Type	Neutron (Bag 1)	Neutron (Bag 2)	Neutron (Bag 3)
FSGL033	30 V	N	1.1×10^{14}	9.9×10^{14}	2.8×10^{15}
FSGL035	60 V	N	1.1×10^{14}	9.9×10^{14}	2.8×10^{15}
FSPL033*	30 V	N	1.1×10^{14}	9.9×10^{14}	2.8×10^{15}
FSL13A0	100 V	N	1.0×10^{13}	1.0×10^{14}	1.0×10^{15}
FSL9130	100 V	P	1.0×10^{13}	1.0×10^{14}	1.0×10^{15}
FSL923A0	200 V	P	1.0×10^{13}	1.0×10^{14}	1.0×10^{15}
2N7397	250 V	N	1.0×10^{13}	1.0×10^{14}	1.0×10^{15}
FSL33A0	400 V	N	1.1×10^{12}	1.1×10^{13}	3.3×10^{13}
FSL430	500 V	N	1.1×10^{12}	1.1×10^{13}	3.3×10^{13}
FRL130	100 V	N	1.0×10^{13}	1.0×10^{14}	1.0×10^{15}
FRL9130	100 V	P	1.0×10^{13}	1.0×10^{14}	1.0×10^{15}
FRL234	250 V	N	1.0×10^{13}	1.0×10^{14}	1.0×10^{15}

Irradiated devices were sent to NAVSEA Crane for electrical characterization, using a Tektronix-370 curve tracer. Measurements consisted of the following DC electrical tests:

- reverse gate-to-source leakage current (I_{GSS}),
- drain-to-source leakage current (I_{DSS}),
- drain-to-source breakdown voltage (BV_{DSS}),
- gate threshold voltage (V_{TH}), and
- drain-to-source on-state voltage (V_{DSON})

Neutrons do not exhibit electrical charge (neutral) and their mass is slightly larger than protons. Therefore, neutrons penetrate deeply into most materials because they do not interact electrically. Displacement damage occurs when a neutron imparts enough energy to displace an atom from its lattice position forming a vacancy. Neutrons can cause significant displacement damage to the atomic lattice and even cause fission reactions, if neutron absorption occurs. Indirect ionization can occur when a neutron collides with the atomic nuclei producing recoils, which then produce ionization along those recoil paths.

Conductivity can be described using the well know expression $\sigma = q\mu N$ where q is electronic charge, μ is majority carrier mobility, and N is the majority carrier concentration. Since mobility is dependent upon the doping concentration and amount of displacement damage, it is expected that displacement damage will effectively decrease the mobility and the effective carrier concentration.

III. TEST RESULTS

Electrical specifications (datasheets) for these devices can be found at <http://www.fairchildsemi.com/products>. Electrical measurements of the different test parameters were performed under similar conditions specified in the datasheets of each tested device type (using commercial protocols).

A. I_{GSS}

Figure 1 displays the averaged gate leakage current (I_{GSS}) of the FSG, FSP, FS, and FR families of the devices tested. All measured values of I_{GSS} currents were between 2.5 to 3.5 nA and none of the devices tested exhibited any notable change in I_{GSS} even after a neutron exposure of 10^{15} neutron \cdot cm $^{-2}$. The maximum allowable specification for I_{GSS} is 100 nA.

B. I_{DSS}

Figure 2 displays the measured drain leakage current of the FSG, FSP, FS and FR families of the devices tested when biased at 40% of the device's rated BV_{DSS} , which resulted in pre-radiation leakage currents between 2 to 4 nA. A significant increase was observed with increasing levels of neutron fluence. This effect is most likely caused by ionization as well as displacement damage. Figure 3 displays the measured drain leakage current when biased at 80% of the device's rated BV_{DSS} , which resulted in pre-radiation leakage currents between 3.5 to 6 nA. Again, a significant increase in leakage current was observed with increasing levels of neutron fluence.

C. BV_{DSS}

As the silicon lattice is neutron irradiated, silicon atoms in the lattice are displaced. These reactions tend to decrease the effective doping of the bulk material and increase the resistivity of the silicon. A decrease in effective doping, in turn, increases the breakdown voltage. Figure 4 displays the drain breakdown voltage response when measured at drain current of 1 mA of the FSG, FSP, FS, and FP families of the devices tested. After neutron irradiation, a notable increase in the breakdown voltage was observed.

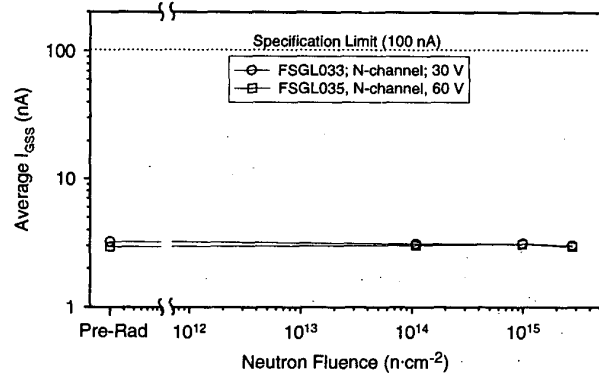


Fig. 1a. I_{GSS} response of the FSG family tested.

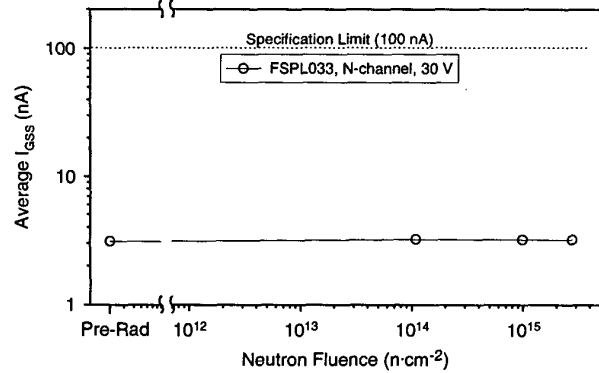


Fig. 1b. I_{GSS} response of the FSP family tested.

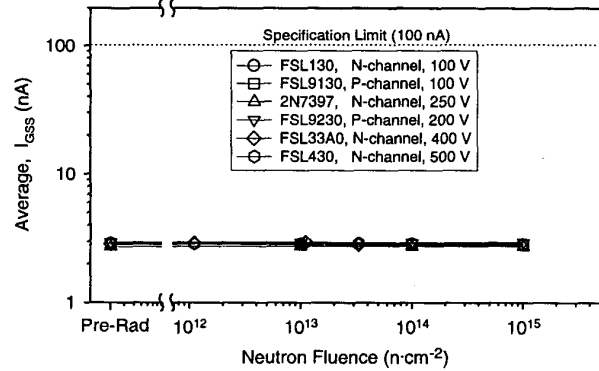


Fig. 1c. I_{GSS} response of the FS family tested.

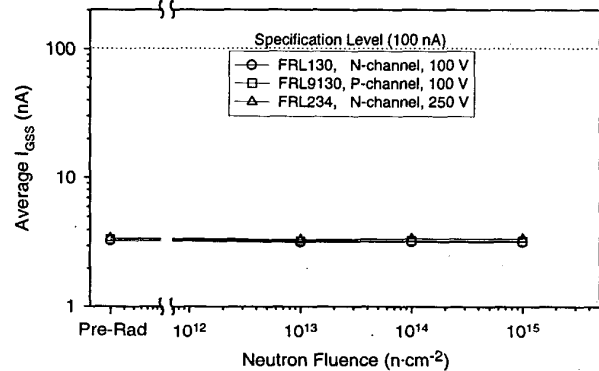


Fig. 1d. I_{GSS} response of the FR family tested.

Fig. 1. Average gate leakage current (I_{GSS}) of the devices tested from the FSG (1a), FSP (1b.), FS (1c.), and FR (1d.) families.

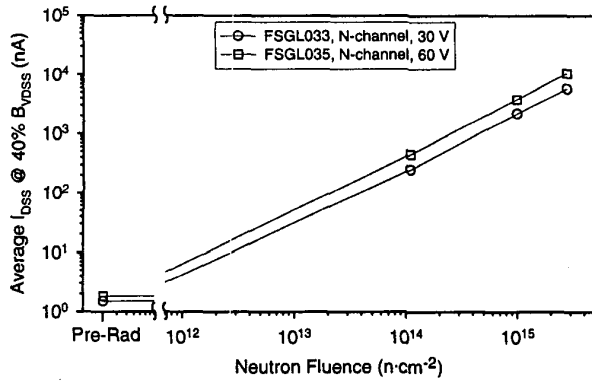


Fig. 2a. I_{DSS} response of the FSG family tested.

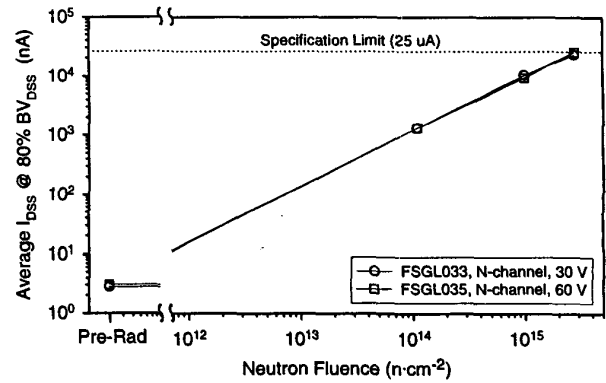


Fig. 3a. I_{DSS} response of the FSG family tested.

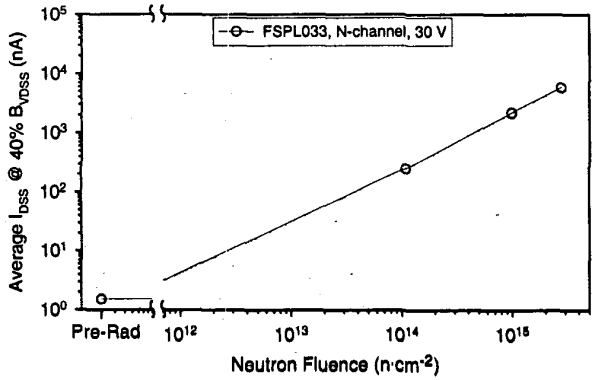


Fig. 2b. I_{DSS} response of the FSP family tested.

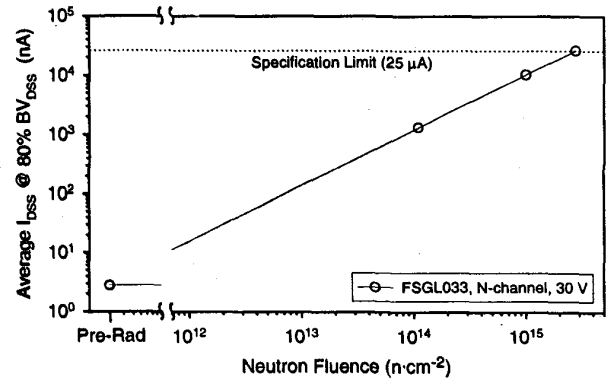


Fig. 3b. I_{DSS} response of the FSP family tested.

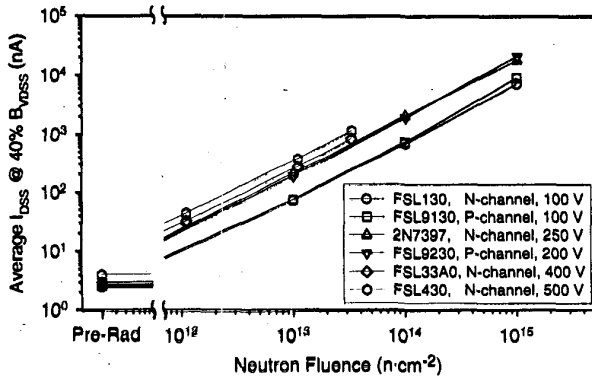


Fig. 2c. I_{DSS} response of the FS family tested.

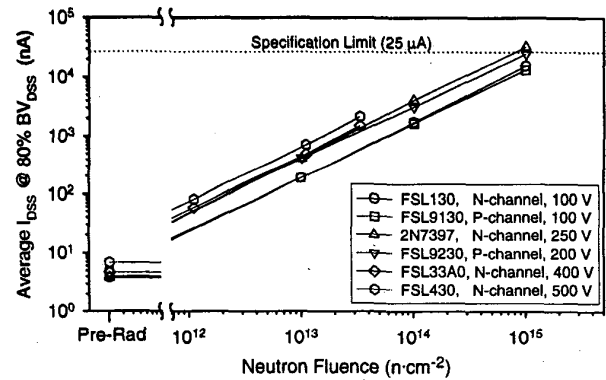


Fig. 3c. I_{DSS} response of the FS family tested.

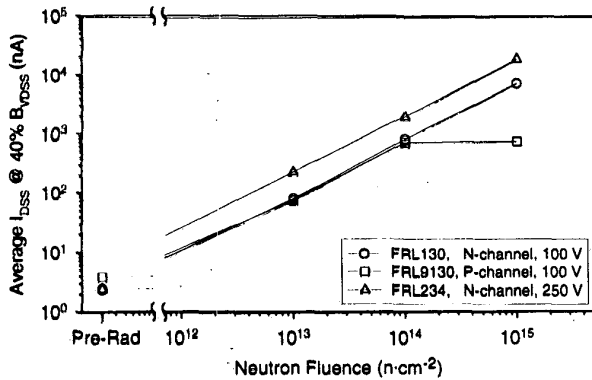


Fig. 2d. I_{DSS} response of the FR family tested.

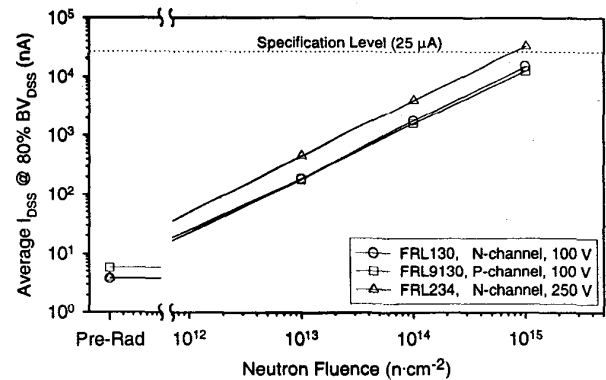


Fig. 3d. I_{DSS} response of the FR family tested.

Fig. 2. Average drain leakage current (I_{DSS}) of the tested devices from the FSG (2a.), FSP (2b.), FS (2c.), FR (2d.) families at 40% of its rated BV_{DSS} .

Fig. 3. Average drain leakage current (I_{DSS}) of the tested devices from the FSG (3a.), FSP (3b.), FS (3c.), FR (3d.) families at 80% of its rated BV_{DSS} .

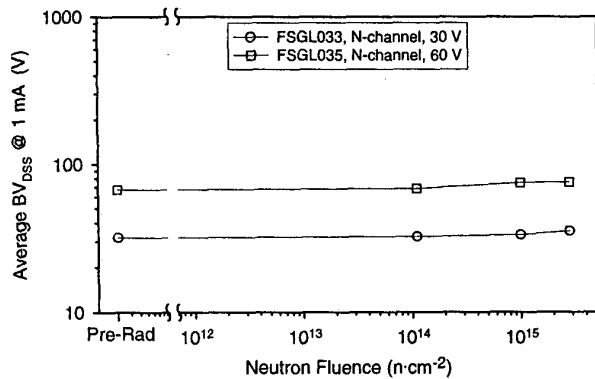


Fig. 4a. BV_{DSS} response of the FSG family tested.

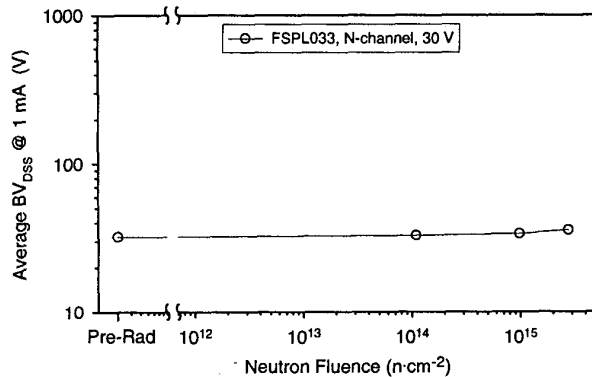


Fig. 4b. BV_{DSS} response of the FSP family tested.

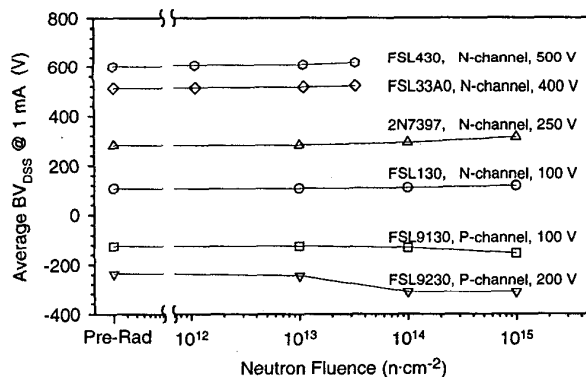


Fig. 4c. BV_{DSS} response of the FS family tested.

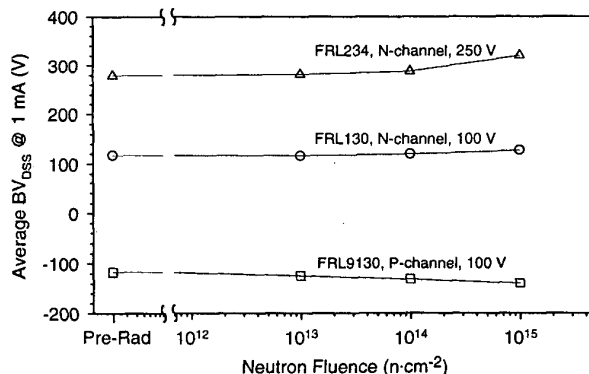


Fig. 4d. BV_{DSS} response of the FR family tested.

Fig. 4. Average drain breakdown voltage (BV_{DSS}) of the tested devices from the FSG (4a.), FSP (4b.), FS (4c.), FR (4d.) families at I_{DS} of 1 mA.

D. VTH

Figure 5 displays the threshold voltage responses when measured at a drain current of 1 mA for N-channel devices and at -1 mA for P-channel devices. Figure 6 displays the threshold voltage responses when measured at a drain current of 5 mA for N-channel devices and at -5 mA for P-channel devices.

For both the N- and P-channel devices, the changes in threshold voltage are consistent with charge build-up in the gate oxide. It is most likely trapped holes induced by gamma radiation, which is incidental to contamination that is present when exposing devices to neutrons. Additional work is planned to separate the trapped charge (N_{OT}) and interface states (N_{IT}), but is not reported here.

E. $R_{DS(on)}$

All $R_{DS(on)}$ measurements were taken using a gate bias of 10 and 12 V for the N-channel devices and a gate bias of -10 and -12 V for the P-channel devices at different I_{DS} values. Figures 7 and 8 present the $R_{DS(on)}$ responses of the FSG L033 and FSG L035 at I_{DS} of 5, 10, and 15 A. Figure 9 presents the $R_{DS(on)}$ response of the FSPL033 at I_{DS} of 5, 10, and 15 A. Figures 10-13 present the $R_{DS(on)}$ responses of the FSL13A0, 2N7397, FSL33A0, and FSL430 at I_{DS} of 2, 3, and 5 A. Figures 14 and 15 present the $R_{DS(on)}$ responses of the FSL9130 and FSL923A0 at I_{DS} of 2, 3, and 5 A. Figures 16-18 present the $R_{DS(on)}$ responses of the FRL130, FRL234, and FRL9130 at I_{DS} of 2, 3, and 5 A.

The on resistance is the electrical parameter, which was most likely to be influenced by displacement damage. Since the on-resistance is strongly dominated by the bulk resistance and this epitaxial layer will sustain a significant amount of displacement damage, the on-resistance is expected to increase significantly. An increase in on-resistance is expected because displacement damage decreases the mobility and effective doping, which, in turn, causes the on-resistance to increase.

It has been known for many years that devices incorporating heavily doped, epitaxial layers (lowers the bulk resistivity) are less sensitive to neutron irradiation than those employing lightly doped epitaxial layers. Therefore, MOS devices with lower breakdowns, which use a heavily doped, epitaxial layer, have less degradation for a given neutron exposure in parameters such as $R_{DS(on)}$ than devices with higher breakdown, which use a lightly doped epitaxial layer. This is graphically shown in Fig. 19. Changes in resistivity were explained by the work of Buehler [1] and later by Messenger and Ash [2].

IV. SUMMARY AND CONCLUSIONS

The data collected in this investigation are in good agreement with the predicted behavior and previously recorded information on neutron irradiation of vertical MOSFET devices. This study was undertaken to revalidate the performance of several radiation-hardened power MOSFET families produced by Fairchild Semiconductor [4], [7]. These data can be used to predict the electrical performance of these devices and similar devices when irradiated to neutrons.

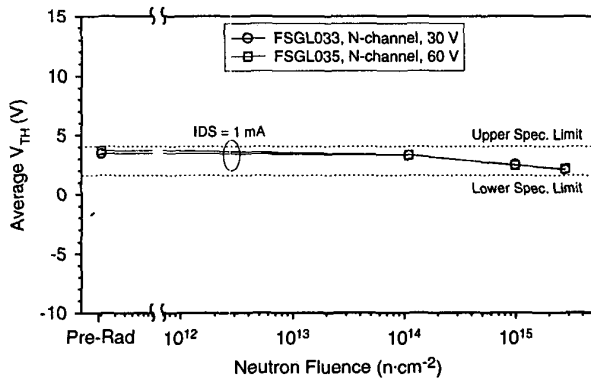


Fig. 5a. V_{TH} response of tested devices from the FSG family.

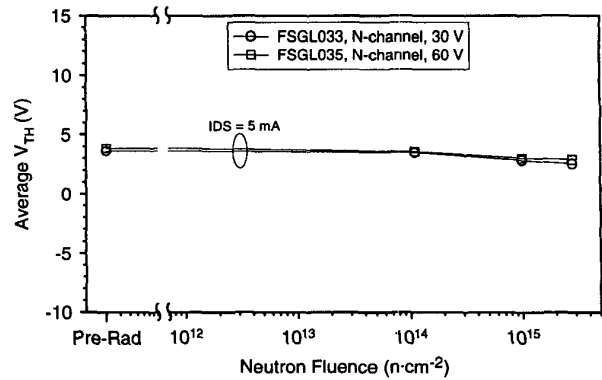


Fig. 6a. V_{TH} response of tested devices from the FSG family.

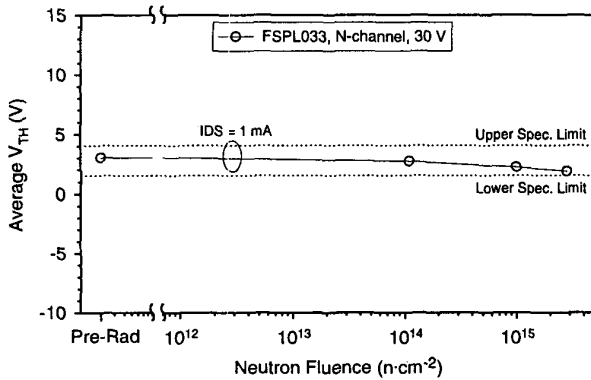


Fig. 5b. V_{TH} response of tested devices from the FSP family.

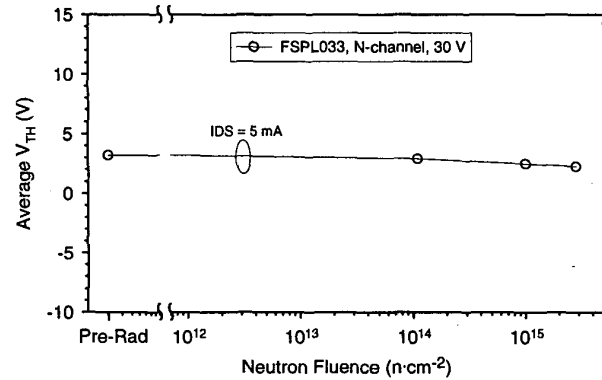


Fig. 6b. V_{TH} response of tested devices from the FSP family.

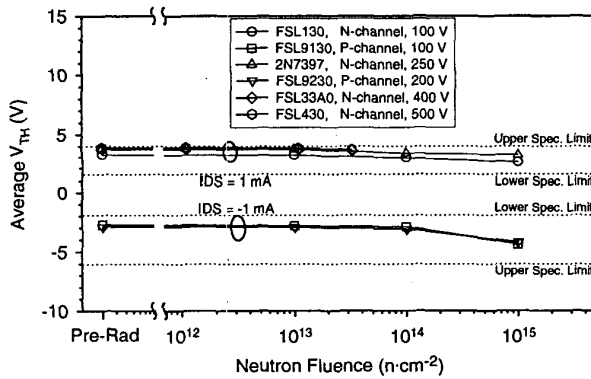


Fig. 5c. V_{TH} response of tested devices from the FS family.

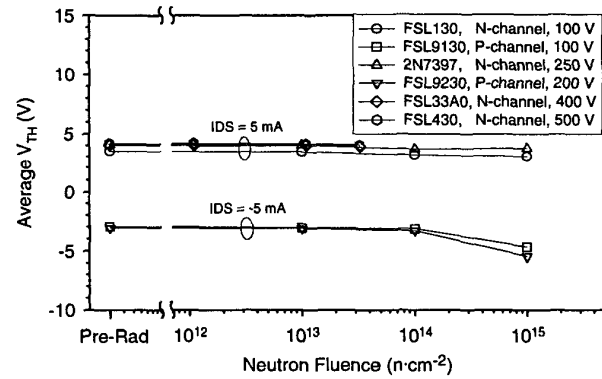


Fig. 6c. V_{TH} response of tested devices from the FS family.

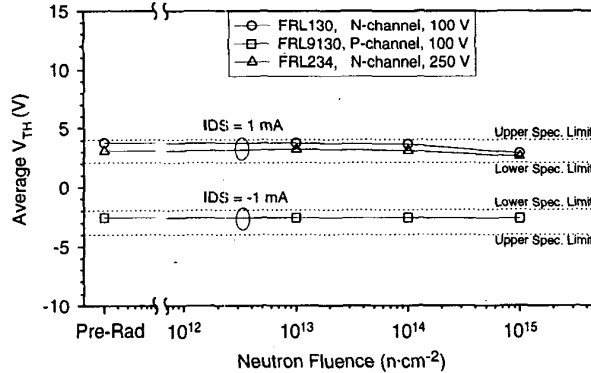


Fig. 5d. V_{TH} response of tested devices from the FR family.

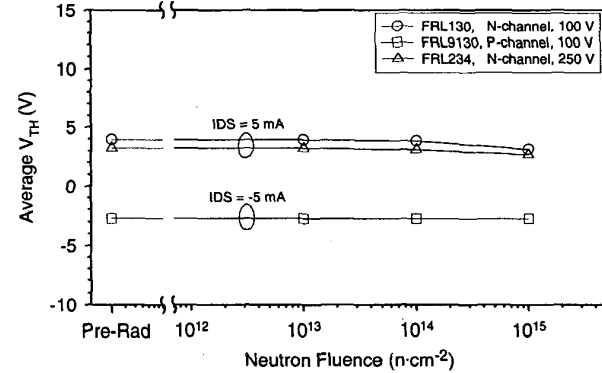


Fig. 6d. V_{TH} response of tested devices from the FR family.

Fig. 5. Average threshold voltage (V_{TH}) of the tested devices from the FSG (5a.), FSP (5b.), FS (5c.), FR (5d.) families at IDS of 1 mA.

Fig. 6. Average threshold voltage (V_{TH}) of the tested devices from the FSG (6a.), FSP (6b.), FS (6c.), FR (6d.) families at IDS of 5 mA.

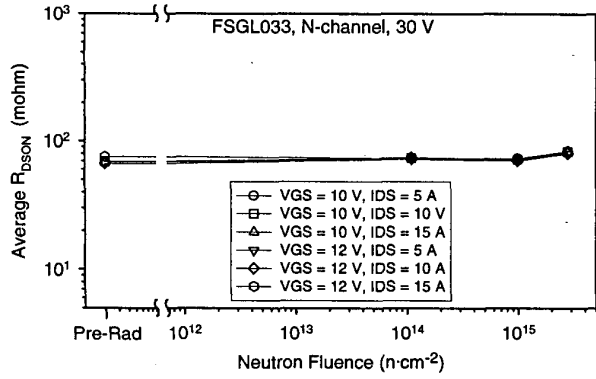


Fig. 7. R_{DSON} responses of the FSGL033.

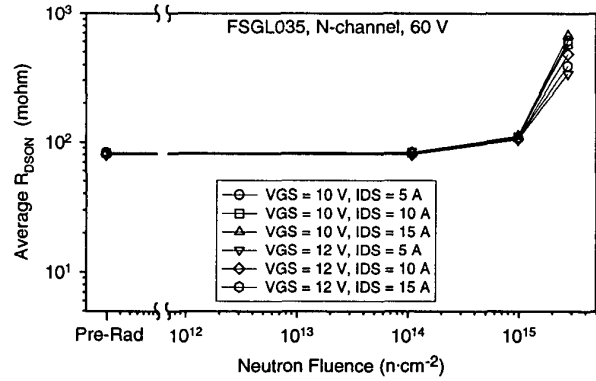


Fig. 8. R_{DSON} responses of the FSGL035 (bottom).

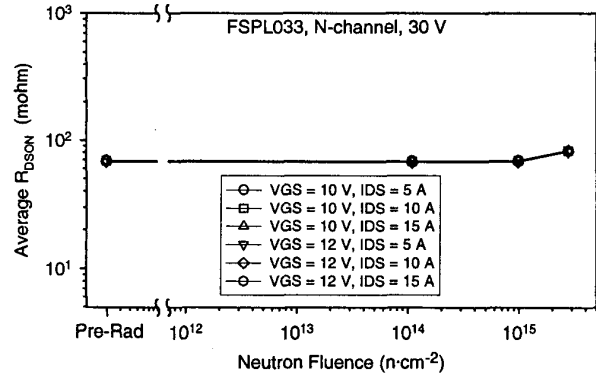


Fig. 9. R_{DSON} responses of the FSPL033.

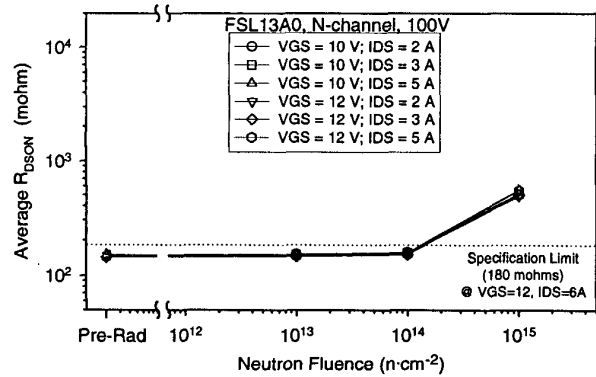


Fig. 10. R_{DSON} responses of the FSL13A0.

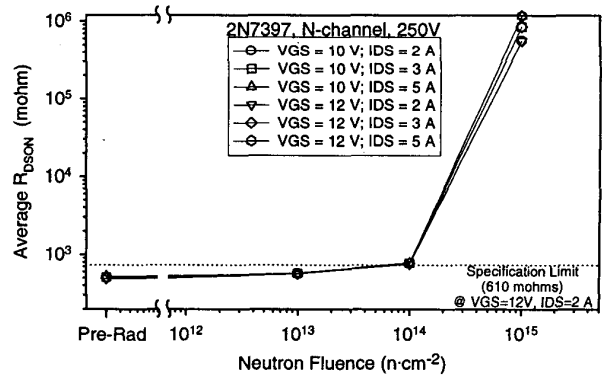


Fig. 11. R_{DSON} responses of the 2N7397.

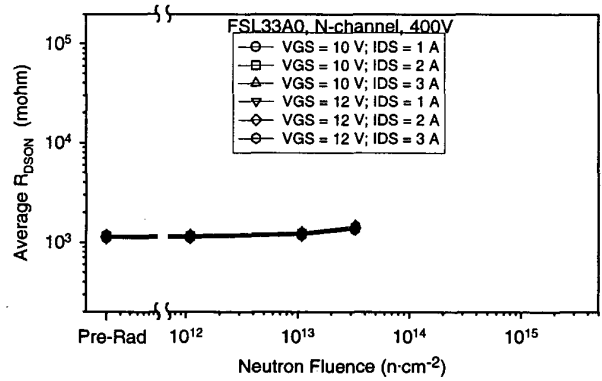


Fig. 12. R_{DSON} responses of the FSL33A0.

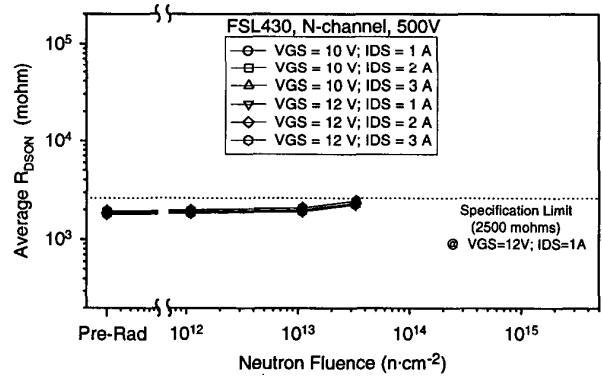


Fig. 13. R_{DSON} responses of the FSL430.

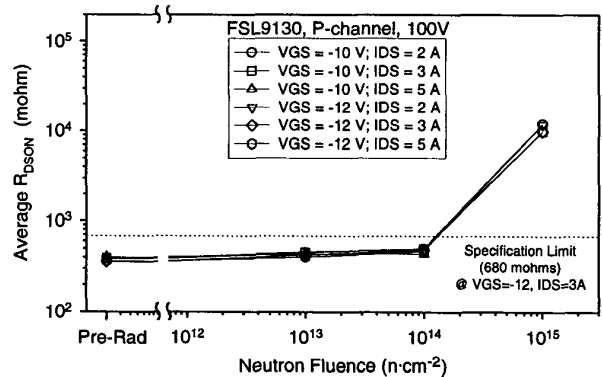


Fig. 14. R_{DSON} responses of the FSL9130.

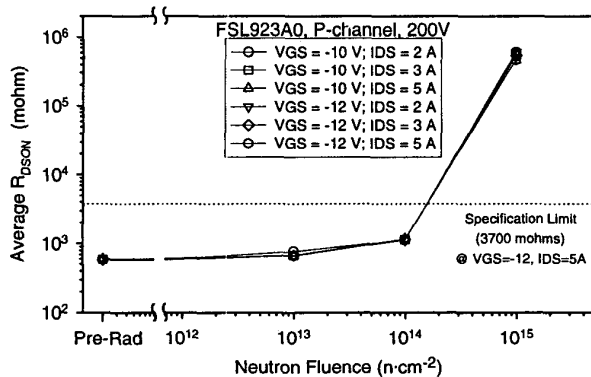


Fig. 15. R_{DSON} responses of the FSL923A0.

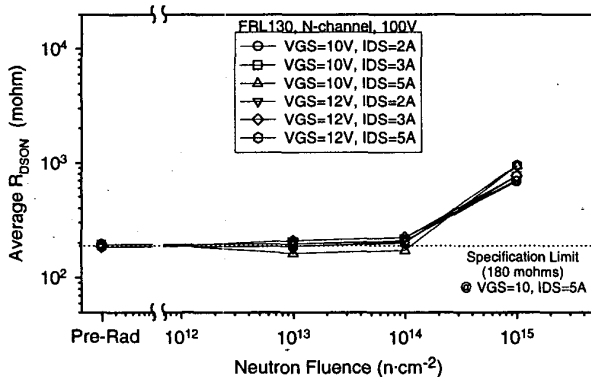


Fig. 16. R_{DSON} responses of the FRL130.

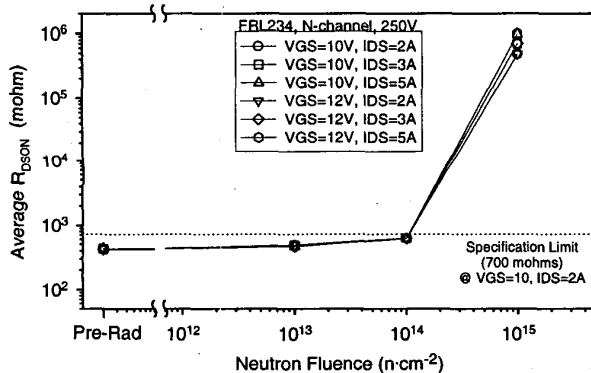


Fig. 17. R_{DSON} responses of the FRL234.

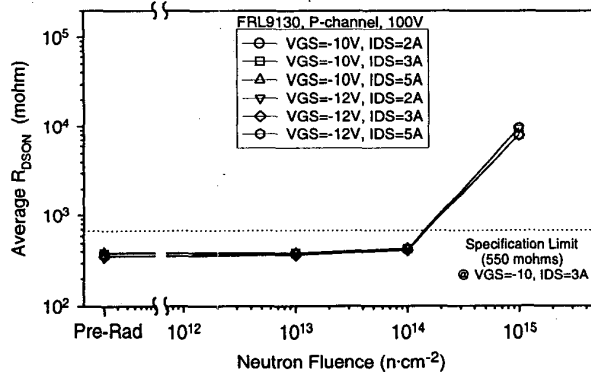


Fig. 18. R_{DSON} responses of the FRL9130.

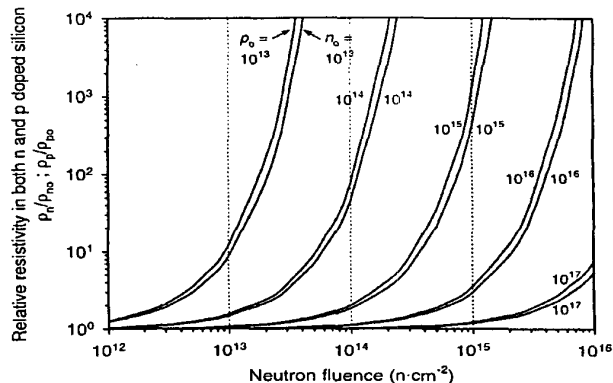


Fig. 19. Relative resistivity of doped silicon [1] and [2].

Key to this revalidation was the establishment that the products performed in excess of their specifications based upon the manufacturers datasheets. Additional products are presently scheduled to undergo irradiation, extending the information to include additional device types from these radiation-hardened families. These data will be included in subsequent reports.

V. ACKNOWLEDGMENT

The authors give special thanks to Fairchild Semiconductor for their program support and the Pennsylvania State University Breazeale TRIGA Mark III nuclear reactor personnel for providing neutron facilities.

VI. REFERENCES

- [1] M. G. Buehler, "Design Curves for Predicting Fast Neutron-Induced Resistivity Changes in Silicon," Proc. IEEE 56, 1741 (1968).
- [2] G. C. Messenger and M. S. Ash, "The Effects of Radiation on Electronic Systems," Von Nostrand Reinhold Company, New York, 1986, p. 200.
- [3] D. L. Blackburn, T. C. Robbins, and K. F. Galloway, "VDMOS Power Transistor Drain-Source Resistance Radiation Dependency," IEEE TNS, Vol. NS-28, No. 6, Dec. 1981, p. 4354-4359.
- [4] C. F. Wheatley, "Radiation Hardening of Vertical DMOS (VDMOS) Power MOSFETs," Harris Semiconductor Sector, Application Note AN-8831, Dec. 1988.
- [5] H. Volmerange & A. A. Witteles, "Radiation Effects on MOS Power Transistors," IEEE TNS, Vol. 29, Dec. 1982, p. 1565-1568.
- [6] G. B. Roper & R. Lewis, "Development of a Radiation Hard N-Channel Power MOSFET," IEEE TNS, Vol. 30, Dec. 1983, p. 4110-4115.
- [7] C. F. Wheatley & L. S. Jamiolkowski, "Development of Radiation Hardened Power MOSFETs," Final Report, Contract # N00164-86-C-0182, Prepared for NAVSEA- Crane, 30 Sep '90.